nature astronomy
SUPPLEMENTARY INFORMATION
https://doi.org/10.1038/s41550-019-0958-x

In the format provided by the authors and unedited.

Cascading parallel fractures on Enceladus

Douglas J. Hemingway[1,2*], Maxwell L. Rudolph[3] and Michael Manga[2]

[1]Department of Terrestrial Magnetism, Carnegie Institution for Science, Washington, DC, USA. [2]Department of Earth & Planetary Science, University of California Berkeley, Berkeley, CA, USA. [3]Department of Earth & Planetary Sciences, University of California Davis, Davis, CA, USA.
*e-mail: dhemingway@carnegiescience.edu

Supplementary Information for "Cascading parallel fractures on Enceladus"

Douglas J. Hemingway*[1,2], Maxwell L. Rudolph[3], Michael Manga[2]

November 18, 2019

[1]Department of Terrestrial Magnetism, Carnegie Institution for Science, Washington, DC, 20015, [2]Department of Earth & Planetary Science, University of California Berkeley, Berkeley, CA, 94720, [3]Department of Earth & Planetary Sciences, University of California Davis, Davis, CA, 95616. *Corresponding author: dhemingway@carnegiescience.edu.

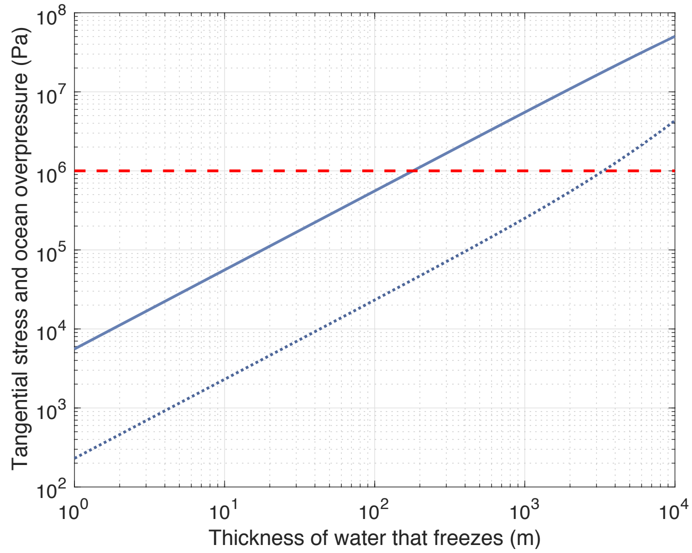

Supplementary Figure 1: Tensile stress accumulation due to ocean freezing — Accumulation of excess ocean pressure (dotted blue line) and the resulting tangential stresses in the ice shell (solid blue line) as a function of the thickness of water that has frozen in the presence of an ice shell that is capable of supporting global tensile stresses. Also shown is a nominal tensile failure limit for cold ice (dashed red line).

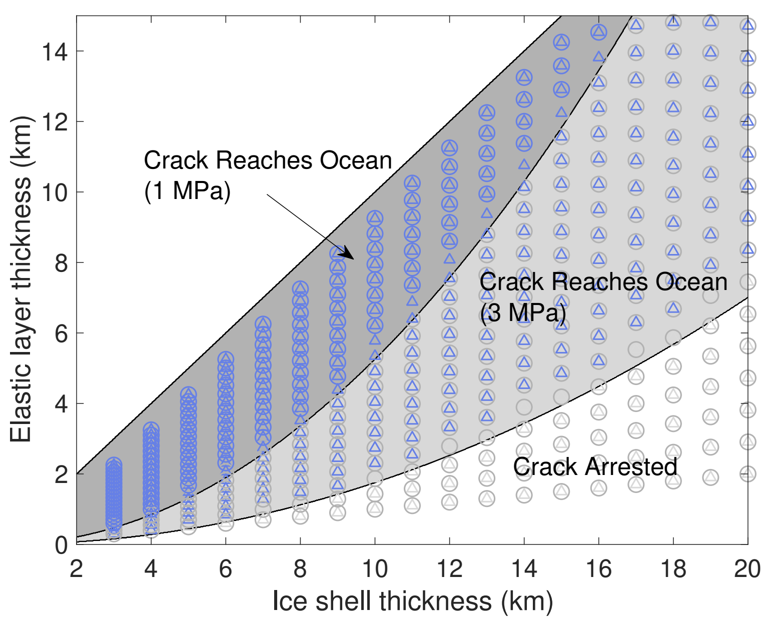

Supplementary Figure 2: Initial fracture penetration — Conditions determining whether or not a fracture initiated at the surface can penetrate entirely through the ice shell, with the dark and light grey regions corresponding to applied stresses of 1 MPa or 3 MPa, respectively, and delineated with the solid black lines given by equation (8), assuming $g = 0.113\,\mathrm{m/s^2}$ and $\rho_i = 930\,\mathrm{kg/m^3}$. The symbols represent the results of the numerical analysis, with blue symbols indicating that the crack reaches the ocean and grey symbols indicating that the crack is arrested; circles and triangles correspond to applied stresses of 1 MPa or 3 MPa, respectively.

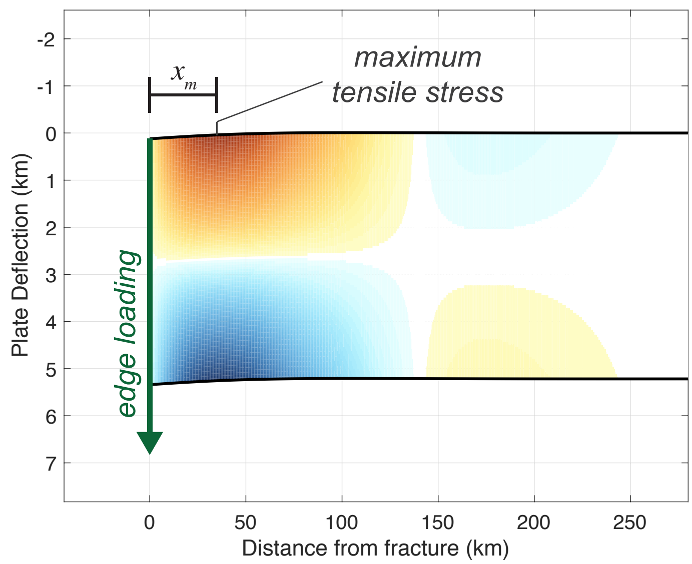

Supplementary Figure 3: Elastic plate deflection and internal stresses — Assumed parameters for this example are $E = 9\,\mathrm{GPa}$, $\nu = 0.25$, $\rho_w = 1020\,\mathrm{kg/m^3}$, and $g = 0.113\,\mathrm{m/s^2}$, for which the elastic thickness required to deliver $x_m = 35\,\mathrm{km}$, given by equations (1) and (2), is $T_e \approx 5.22\,\mathrm{km}$. Deflection is computed according to equation (12) and is shown without any vertical exaggeration (though note that the illustration's aspect ratio is approximately 30:1). Fibre stresses are computed with equation (16) and are illustrated with shading, where warm colours correspond to tensile (positive) stresses and cool colours to compressive (negative) stresses. Compressive stresses due to overburden pressure are not shown. In the example illustrated, the deflection at the edge of the plate reaches a maximum value of $\approx 120\,\mathrm{m}$ when the maximum fibre stress reaches $1\,\mathrm{MPa}$.

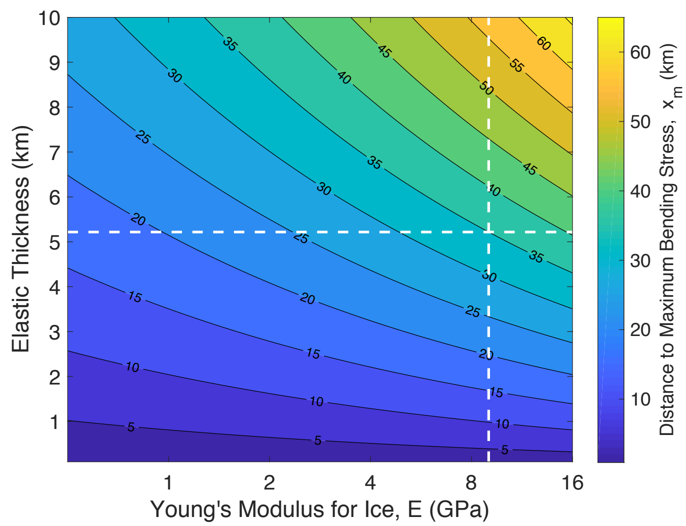

Supplementary Figure 4: Position of maximum tensile stress — Distance from the fracture to the position of maximum tensile stress, computed via equation (15), as a function of the ice shell's elastic properties: namely the Young's modulus (E, shown on a logarithmic scale) and the effective elastic layer thickness (T_e). A fixed Poisson's ratio of $\nu = 0.25$ is assumed. As a point of reference, a nominal Young's modulus of $E = 9\,\mathrm{GPa}$ is indicated with a vertical dashed white line, illustrating that the spacing of $35\,\mathrm{km}$ corresponds to an elastic thickness of $T_e \approx 5.2\,\mathrm{km}$, indicated by the horizontal dashed white line.

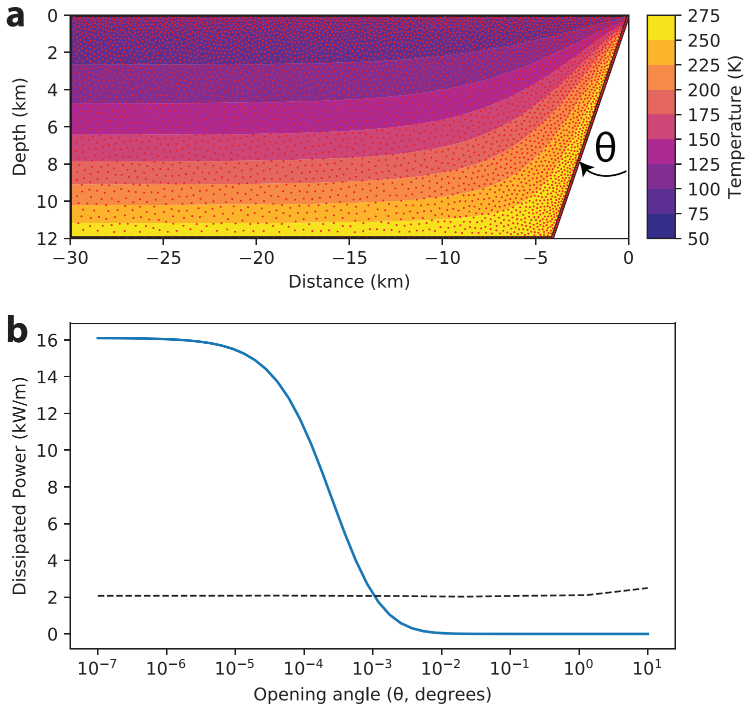

Supplementary Figure 5: Melt-back wedge development — (a) Development of ice shell temperature structure in the vicinity of a liquid filled fissure. The red dots represent the evaluation points in the radial basis function calculation. (b) Turbulent dissipation as a function of the fissure's opening angle, θ. The dashed black line indicates the approximate dissipation required to keep the fissure from freezing shut. For opening angles larger than $\sim 10^{-3}$ degrees, the dissipation is not sufficient to keep the fissure open.

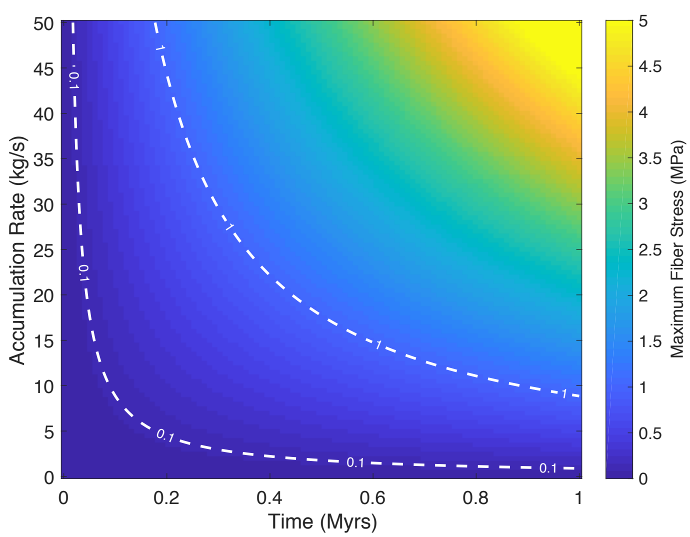

Supplementary Figure 6: Stress accumulation due to ridge loading — Accumulated tensile stresses at $x_m = 35\,\mathrm{km}$ as a function of time and the rate of material accumulation in the flanking ridge, whose length is assumed to be 100 km. The dashed white contours illustrate failure envelopes assuming tensile failure limits of 100 kPa or 1 MPa.

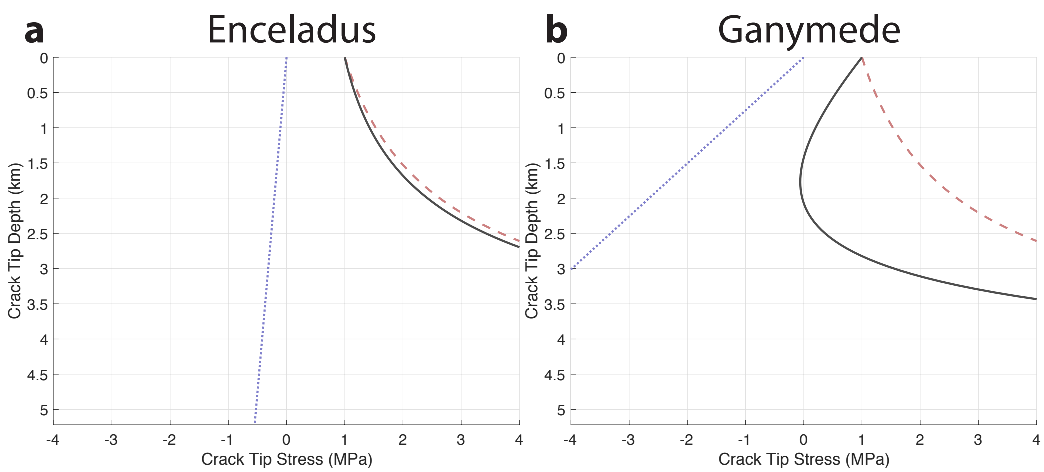

Supplementary Figure 7: Crack tip stress resulting from bending — Stresses at the crack tip as a function of crack tip depth for the cases of (a) Enceladus and (b) Ganymede. Positive stresses are tensile, negative stresses are compressive. The dotted blue line represents the compressive stresses due to lithostatic pressure. The dashed red line represents the bending stresses given by equation (29). The solid black line represents the net stress given by equation (30). Whereas for Enceladus, the crack tip stress is always increasing as the crack propagates downward, the crack tip stress initially decreases for Ganymede, even when we assume an equally thin ice shell. The surface gravity is $g = 0.113\,\mathrm{m/s^2}$ for Enceladus and $g = 1.428\,\mathrm{m/s^2}$ for Ganymede. For both examples, we assume $T_e = 5.2\,\mathrm{km}$, $\sigma_{\mathrm{crit}} = 1\,\mathrm{MPa}$, and $\rho_{\mathrm{ice}} = 930\,\mathrm{kg/m^3}$.